



Technical Note

Deriving the mean excitation energy map from dual-energy and proton computed tomography[☆]Gloria Vilches-Freixas^{*}, Catherine Therese Quiñones¹, Jean Michel Létang, Simon Rit^{**}

Univ Lyon, INSA-Lyon, Université Claude Bernard Lyon 1, UJM-Saint Étienne, CNRS, INSERM, CREATIS UMR 5220, U1206, Centre Léon Bérard, F-69373 Lyon, France

ARTICLE INFO

Keywords:
Proton CT
Dual-energy CT
Mean excitation energy

ABSTRACT

The mean excitation energy, I , is an essential quantity for proton treatment planning. This work investigated the feasibility of extracting the spatial distribution of I by combining two computed tomography (CT) modalities, dual-energy CT and proton CT, which provided the spatial distribution of the relative electron density and the stopping power relative to water, respectively. We provided the analytical derivation of I as well as its uncertainty. Results were validated on simulated X-ray and proton CT images of a digital anthropomorphic phantom. Accuracy was below 15% with a large uncertainty, which demonstrated the potential and limits of the technique.

1. Introduction

The mean excitation energy, sometimes referred to as the average ionization potential and noted I in the following, is an essential parameter for proton treatment planning but controversial as there is no consensus on how to establish reference values for different media. Although I is a well-defined quantity for a given material and it only depends on the properties of the medium [1], there are large uncertainties associated to its determination. Elemental I is generally derived from experimental data [1] such as stopping-power or range measurements for several charged particle beams, but there is limited experimental data for compounds and mixtures except water. Moreover, even for liquid water, which is highly investigated, there is no consensus on the mean excitation energy [2] with variations up to 20%, and values deduced from experiments are higher than theoretical derivations [3]. Experimental values for water range between 75 eV [4] and 81.8 eV [5] and recommended values range from 67.2 eV (ICRU Report 73 [6]) to 78 eV (Errata ICRU Report 73 [7]) with 75 eV in between (ICRU Reports 37 [8] and 49 [1]). When the I value of a medium is not known, it is computed by Bragg's additivity rule based on its tabulated chemical composition and mass density. As this rule is an approximation and it ignores the effects of chemical bonds, I estimates of human tissues have large uncertainties (up to 15%) [8,9]. The available reference human tissue compositions [10–13] are average values obtained under different conditions and are expected to be

approximate [9]. Moreover, there is a large variability on I values of similar human tissues reported in publications of the International Commission on Radiation Units (ICRU) [8,12,14]. There is currently no solution to image the spatial distribution of I in a heterogeneous object (e.g. a patient). In this work, we evaluate the feasibility of an experimental setup designed to derive the I map by combining two computed tomography (CT) imaging modalities: dual-energy CT (DECT) and proton CT.

2. Materials and methods

2.1. Phantom

The adult female (AF) reference computational phantom of the International Commission on Radiological Protection (ICRP) [13] was selected as a virtual patient. This anthropomorphic phantom represented an average female subject divided into 140 organs made of 52 standard human tissues, with known mass densities and chemical compositions. It had voxel dimensions of $1.775 \times 1.775 \times 4.84 \text{ mm}^3$. For this study, three slices were selected at different locations: head, thorax and pelvis.

2.2. RED determination

Virtual X-ray CT acquisitions of the AF phantom were obtained

[☆] Deriving I map from DECT and pCT.

^{*} Corresponding author at: MAASTRO Clinic, Dr. Tanslaan 12, 6229 ET Maastricht, The Netherlands.

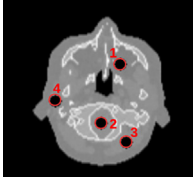
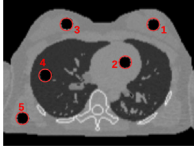
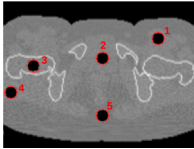
^{**} Principal corresponding author.

E-mail addresses: Gloria.VilchesFreixas@maastro.nl (G. Vilches-Freixas), Jean-Michel.Letang@creatis.insa-lyon.fr (J.M. Létang), Simon.Rit@creatis.insa-lyon.fr (S. Rit).

¹ Present address: Department of Physics, Mindanao State University – Iligan Institute of Technology, Iligan City, Philippines.

Table 1

Quantitative evaluation of I in the ROIs drawn in the first column on top of RED images. The relative I error (last column) is obtained as the difference of the measure with the reference divided by the reference.

	ROI	Tissue	RED (unitless)		SPR (unitless)		I (eV)		σ_I (eV) Eq. (4)	I error (%)
			Ref.	$\mu \pm \sigma$	Ref.	$\mu \pm \sigma$	Ref.	Med $\pm \sigma$		
	1	Adipose	0.95	0.95 \pm 0.02	0.97	0.97 \pm 0.02	63	60 \pm 13	14	-5.0
	2	Brain	0.04	1.05 \pm 0.02	1.06	0.06 \pm 0.02	69	71 \pm 20	17	3.0
	3	Muscle	1.04	1.04 \pm 0.02	1.05	1.05 \pm 0.02	69	74 \pm 14	15	7.2
	4	Salivary gland	1.02	1.02 \pm 0.02	1.04	1.04 \pm 0.02	68	67 \pm 15	14	-1.2
	1	Mammary gland	1.02	1.02 \pm 0.02	1.04	1.05 \pm 0.02	64	62 \pm 20	22	-3.1
	2	Blood	1.05	1.05 \pm 0.02	1.06	1.06 \pm 0.02	70	70 \pm 24	21	0.8
	3	Mammary gland	1.02	1.02 \pm 0.02	1.04	1.04 \pm 0.02	64	65 \pm 24	21	1.6
	4	Compressed lungs	0.38	0.38 \pm 0.02	0.39	0.39 \pm 0.02	70	54 \pm 46	49	-21.8
	5	Muscle	1.04	1.03 \pm 0.04	1.05	1.04 \pm 0.04	69	65 \pm 36	37	-6.9
	1	Muscle	1.04	1.04 \pm 0.03	1.05	1.05 \pm 0.03	69	67 \pm 29	30	-2.9
	2	Urine	1.03	1.03 \pm 0.05	1.05	1.04 \pm 0.05	70	60 \pm 37	33	-14.5
	3	Femora spongiosa	1.04	1.03 \pm 0.05	1.06	1.05 \pm 0.05	67	62 \pm 39	36	-7.1
	4	Muscle	1.04	1.05 \pm 0.05	1.05	1.06 \pm 0.05	69	78 \pm 38	47	-12.3
	5	Adipose	0.95	1.95 \pm 0.04	1.97	0.98 \pm 0.04	63	59 \pm 37	35	-6.5

using deterministic simulations in Gate v7.2 [15]. The DECT spectra employed in the simulation were 80 kV and 140 kV + 0.4 mm Sn which corresponds to the Siemens Flash spectra [16]. The simulated detector response was accounted for in the deterministic simulation by weighting each source spectrum by the detector response. Poisson noise was applied to the projections corresponding to a central dose of about 20 mGy with the DECT acquisition while keeping a balanced dose between the low and the high energy acquisitions, as described in [17]. The basis material decomposition method proposed in [18] was implemented in the projection domain to extract the relative electron density (RED) map. The RED image was reconstructed using filtered backprojection with $380 \times 380 \times 1$ voxels of size $1 \times 1 \times 1$ mm³. For further details on the DECT simulations and the RED reconstruction, the reader is referred to [19].

2.3. SPR determination

The proton CT scanner described in [20] was simulated using the same Gate v7.2. The conceptual design of the simulated scanner consisted of two ideal detectors, one before and one after the phantom, measuring the position, the direction and the energy of each proton (list-mode). An incident proton beam of 300 MeV was used, which is sufficient for the proton beam to pass through in any direction of the three selected slices of the AF phantom. The delivered dose was recorded during the Gate simulation from the energy deposition in a voxelized map aligned with the ICRP lattice and it was about 5 mGy. The effect of multiple Coulomb scattering was mitigated by estimating the most likely path of each proton from the measured positions and directions following [21] and including it in a filtered backprojection reconstruction algorithm [20]. Stopping power relative to water (SPR) images were reconstructed on a $380 \times 380 \times 1$ mm³ lattice like the DECT images. Protons which underwent nuclear interactions were filtered out using 3σ cuts on the exit energy and angular distributions before image reconstruction [21]. For further details on the proton CT scanner simulation and the SPR reconstruction, the reader is referred to [22].

2.4. I determination

The I map was estimated based on Bethe's equation without correction terms [23]

$$S = 4\pi r_e^2 m_e c^2 \rho_e \frac{z^2}{\beta^2} \left(\ln \frac{2m_e c^2 \beta^2}{I(1-\beta^2)} - \beta^2 \right) \quad (1)$$

where S is the stopping power of the medium, r_e the classical electron radius, m_e the mass of an electron, c the speed of light in vacuum, ρ_e the electron density of the medium, z the charge of the projectile, and $\beta = v/c$ with v the velocity of the projectile.

The mean excitation energy of the object was computed pixel-by-pixel by computing

$$I(\mathbf{x}) = \frac{2m_e c^2 \beta^2}{1-\beta^2} \exp \left(- \frac{\text{SPR}(\mathbf{x})}{\text{RED}(\mathbf{x})} \left(\ln \frac{2m_e c^2 \beta^2}{I_w(1-\beta^2)} - \beta^2 \right) - \beta^2 \right) \quad (2)$$

with $\text{SPR} = S/S_w$ the stopping power ratio and S_w the stopping power of water, I_w the mean excitation energy of water, which was set to 78 eV in Geant4, and $\beta^2 = 0.43$ corresponding to an energy of 300 MeV. This latter choice outlines the energy dependence of Eq. 2 which stems from the energy dependence of S propagating to the SPR. It can easily be seen that there is no energy dependence when $\text{SPR}/\text{RED} = 1$, i.e., for water. For other tissues, the calculated I will depend on the choice of the energy-dependent β . However, for human tissues, the SPR variations are small in the 80–300 MeV energy range [24]. For the AF tissues, the difference between I values for $\beta^2 = 0.18$ (100 MeV) and $\beta^2 = 0.43$ (300 MeV) was at maximum 6.1% (for the teeth) and below 1% for 44 of the 52 tissues.

2.5. Uncertainty of I

The uncertainty of I computed from SPR and RED using Eq. (2) was calculated using the first-order Taylor series expansion known as the propagation of uncertainty. We assumed that RED and SPR were independent variables since they were computed from independent measurements. The variance of σ_I^2 was then given by

Download English Version:

<https://daneshyari.com/en/article/8919578>

Download Persian Version:

<https://daneshyari.com/article/8919578>

[Daneshyari.com](https://daneshyari.com)